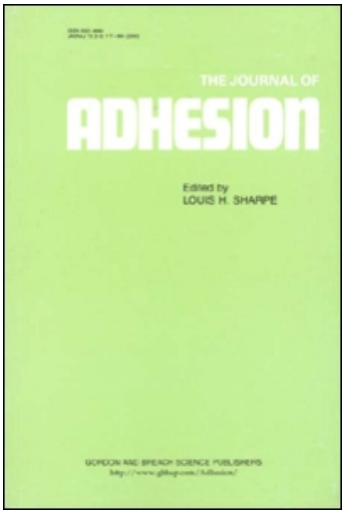

The Journal of Adhesion
Publication details, including instructions for authors and subscription information:
http://www.informaworld.com/smpp/title~content=t713453635

Asymptotic Fields in Adhesive Fracture

Roshdy S. Barsoum[ab]
[a] US Army Materials Technology Laboratory, Watertown, MA, U.S.A. [b] Solid Mechanics Program, Office of the Chief of Naval Research, Arlington, VA, U.S.A.

To cite this Article Barsoum, Roshdy S.(1989) 'Asymptotic Fields in Adhesive Fracture', The Journal of Adhesion, 29: 1, 149 — 166
To link to this Article: DOI: 10.1080/00218468908026485
URL: http://dx.doi.org/10.1080/00218468908026485

J. Adhesion, 1989, Vol. 29, pp. 149–166
Reprints available directly from the publisher
Photocopying permitted by license only

Printed in the United Kingdom

Asymptotic Fields in Adhesive Fracture†

ROSHDY S. BARSOUM*

US Army Materials Technology Laboratory, Watertown, MA 02172, U.S.A.

(Received August 1988; in final form February 24, 1988)

This paper presents the asymptotic singular fields associated with the fracture analysis of adhesive joints and the micromechanics of adhesive failure. The fracture parameters used in adhesives are examined and their validity and use in applications is evaluated. Contrary to conventional fracture mechanics of homogeneous media the asymptotic field in most adhesive fracture is a function of the following: the adhesive and adherend properties, the dimensionality of the crack geometry, and their relationship to the interface. The Finite Element Iterative Method (FEIM) is used in analyzing the asymptotic fields. The results of the singularities for interfacial cracks of various geometries and material properties are presented and discussed in relation to adhesive failures.

KEY WORDS Finite element iterative method (FEIM); interface cracks; fracture analysis of adhesives; micromechanics; singularities; bimaterial interfaces, adhesive joints.

INTRODUCTION

Currently, most adhesive fracture testing standards and fracture analysis rely heavily on concepts and analysis methods which were developed for the fracture of homogeneous materials, even though the adhesive-adherend continuum is nonhomogeneous. Some of the adhesive fracture parameters are specimen and geometry dependent and, therefore, are not purely material properties as in the case of homogeneous materials. In addition, some of the adhesive analysis methods, e.g. in Finite Element Analysis, lead to incorrect interpretation of the test results, because of a modeling dependence issue.

Recent advances in the analysis of cracks at bimaterial interfaces has increased the understanding of the elastic as well as the inelastic fracture behavior at, or near, interfaces. The new finite element approaches to fracture analysis of interfaces have provided for the characterization of the asymptotic fields and the

* Present address: Solid Mechanics Program, Office of the Chief of Naval Research, Code 1131, 800 North Quincy Street, BCT #1, Arlington, VA 22217-5000, U.S.A.
† Presented at the 35th Sagamore Army Materials Research Conference, Manchester, New Hampshire, U.S.A., June 26–30, 1988.

determination of the associated fracture parameters that are only material dependent.

This paper discusses the results obtained using the Finite Element Iterative Method (FEIM)[1–4] in determining linear and nonlinear asymptotic singularity fields of interfacial cracks of various geometries. Cracks at bimaterial interfaces, cracks inclined to interfaces, and cracks at corners, are included in the analysis. A discussion of some of the problems encountered in current testing of adhesives and the possible explanation for such discrepancies is also to be presented.

The micromechanics and nonlinear effects in adhesive fracture are described as they relate to the results from the asymptotic fields computations.

I FRACTURE TESTING OF ADHESIVE JOINTS AND VARIATIONS IN ENERGY RELEASE RATES

Different types of test specimens are used for determining the fracture toughness of adhesives, which depends on the application and the mode of failure. Some of the specimen geometries are a derivative of those used in the fracture testing of homogeneous materials.

The Mode II fracture specimens are mostly based on the lap shear test, or a modification thereof, which is given in the ASTM standards. The end-notch specimen, loaded as a cantilever beam or 3-point bend beam, has recently gained popularity for Mode II because of its possibility for mixed-mode testing. The Iospiescu[5] and Arcan[6] test fixtures have also been used for Mode II and the latter also Mode I and mixed mode. Ref. 7 uses a so-called independently-mixed mode loaded specimen (IMMLs), which may not be a great deal different from one of the above tests.

Most of the above test specimens are used for the evaluation of the strain energy release rates G_I and G_{II}, which are calculated from a compliance method or some other load/displacement measurement. The energy release rates reported by different investigators for both Modes I and II show a large scatter in the data. For example, Ref. 7, using IMMLs, shows for Metlbond 1113-2, adhesive (Narmco) that G_{Ic} could vary from 2 to 15 in-lb/in^2 for a fixed $G_{II} = 1.5$ in-lb/in^2. Similarly, that G_{IIc} could vary from 0.8 to 1.7 in-lb/in^2 for a fixed $G_I = 15$ in-lb/in^2. The authors of Ref. 8 used the end-notch specimen in evaluating the fracture of FM300 adhesive (American Cyanamid). The results indicated that G_{Ic} and G_{IIc} measurements depend on the crack length and loading. In most cases the scatter in Mode II fracture was quite significant. In this case, the authors attributed the scatter to nonlinearities.

It could also be argued that the scatter is due to nonuniformity of specimen fabrication procedures. However, similar scatter is observed in the results obtained by many other investigators. For example, Ref. 9 shows scatter in the results of fatigue crack growth of a mixed-mode adhesively bonded cracked-lap-shear specimen. The authors argue that the scatter they observe is of the order of 7, which is similar to fatigue crack growth results in metals. The fact is that such scatter in metals is observed over all results obtained from various investigators,

manufacturers and test specimens, and not for a single investigator and a single type of test specimen. In addition, if one compares results from the two loading cases in Ref. 9, one can conclude that the scatter is much greater than was reported in the paper.

The results reported in Ref. 10 on the effect of high relative humidity and high temperature on the fracture of adhesive showed large scatter. In this investigation a compact tension specimen was used and G_c was calculated using a standard ASTM compliance method. Due to the large scatter in the results, the study concluded that G_c does not fully characterize the fracture toughness of these moisture-resistant and high-temperature epoxy adhesives.

In conclusion, the energy release rates as calculated from the test results discussed above are not purely material properties, but depend on specimen geometry, adhesive thickness, degree of mixed mode and on adherend properties. The scatter in the results of G_{Ic} and G_{IIc} is contrary to results of fracture mechanics in homogeneous media, which presents a profound problem to any design methodology for adhesives that uses fracture mechanics concepts. The use of standard statistical methods in obtaining G_{Ic} and G_{IIc} design allowables would produce extremely low values, thus erroneously identifying a minuscule load-carrying capacity of the adhesive joint. This is not the case, as these adhesives are being used by various industries, including airframe manufacturers, which implies that their load-carrying capacity is acceptable even with the existence of flaws.

It is the author's opinion that the direct application of fracture parameters that are obtained from the fracture mechanics of homogeneous material represents a gross simplification of the fracture process in adhesive materials. One of the factors that contributes to the scatter in the strain energy release rate results is that mixed modes always exist whenever the fracture is at, or near, an interface. The calculation of energy release rate at an interface requires a knowledge of its asymptotic field, which will be given in the following sections. Other factors include the existence of mixed cohesive and adhesive failure in addition to material nonlinearities. The asymptotic fields for these cases will also be described in the text.

II MICROMECHANICS OF FRACTURE IN ADHESIVES

In order to assess the large variability in G_{Ic} and G_{IIc} testing, the micromechanics of failure should be studied. In adhesive failure, micromechanics of fracture refers to the quantitative evaluation of crack propagation which includes cohesive and adhesive modes and interactions at the interfaces with the adherend. Figure 1 shows the manner in which an investigation could proceed in examining crack propagation from cohesive to adhesive failure, from mode I to mode II to mixed mode. The major difficulty in performing such an analysis and, in addition, determining the associated fracture parameters, involves the solution of the asymptotic singular field at the interfaces at the locations shown in Figure 1. The asymptotic field refers to the stress field near a singularity point, e.g. a crack tip, as the distance from that point approaches zero.

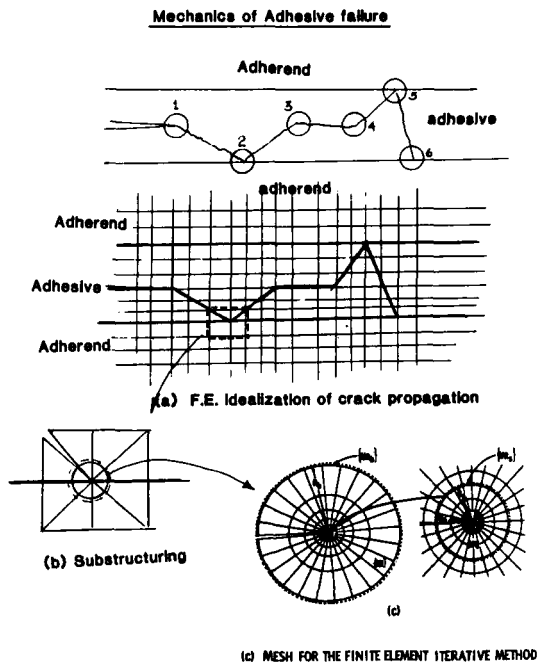

FIGURE 1 Micromechanics analysis of adhesive failure. (a) Finite element idealization of cohesive–adhesive crack propagation. (b) Substructuring for FEIM. (c) Mesh for the finite element iterative method (FEIM).

III NONLINEAR MATERIAL BEHAVIOR EFFECTS IN ADHESIVE FRACTURE

Kinloch and Shaw[11] have shown qualitatively that for a toughened epoxy adhesive the size of the plastic zone can be related to the adhesive thickness which, in turn, correlates with the values of G_{Ic}. This conclusion, in addition to the arguments discussed above regarding the dependence of the energy release rates on the crack length,[8] show the need for consideration of asymptotic fields for the two cases of cohesive and adhesive cracks shown in Figure 2.

The plastic zone associated with cohesive failure can be described by the HRR-singularity field.[12,13] However, the plastic zone associated with adhesive failure, Figure 2b, has no analytical solution. A numerical solution for this case was recently obtained using the Finite Element Iterative Method.[14] Using FEIM, the results for adhesives with power law hardening behavior are presented in this paper.

IV SINGULARITIES IN ADHESIVE JOINT

The asymptotic singularity field for many cases of adhesive fracture are not available due to the complexity of the analytical formulations, and lack of their

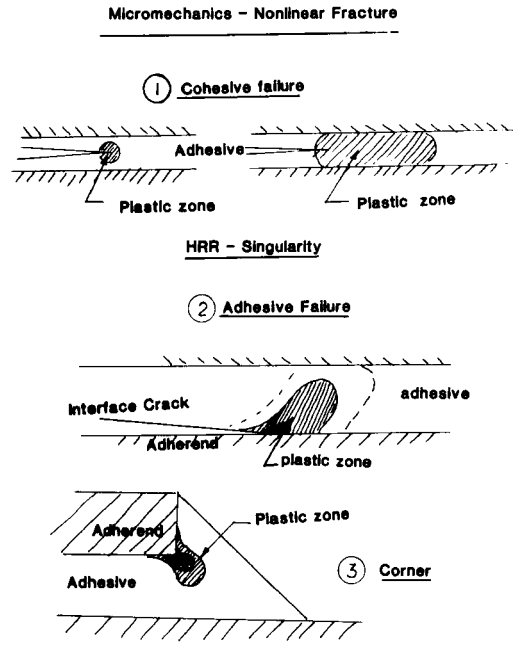

FIGURE 2 Nonlinear effects in the micromechanics of adhesive fracture. (a) Cohesive failure. (b) Adhesive failure (c) Other singularities—(corner singularity).

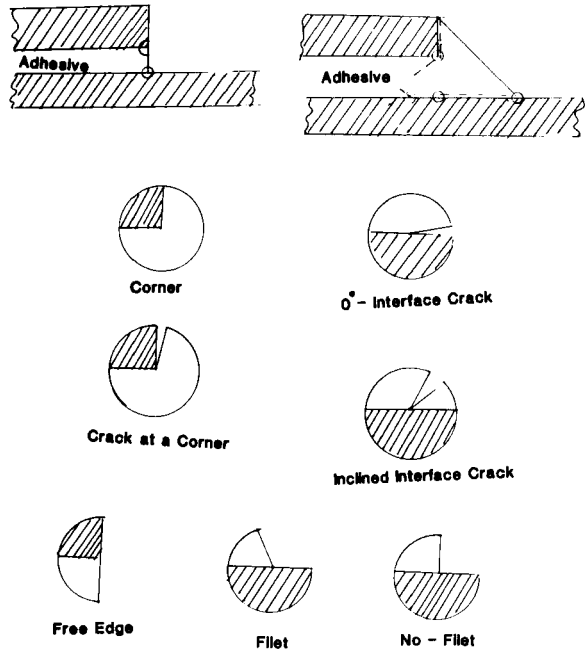

FIGURE 3 Singularities in adhesives.

generality. There is a need for investigating adhesive fracture at interfaces which accounts for material anisotropy as well as inelastic behavior. Figure 3 shows some of the geometries which will be discussed here. They involve interfacial cracks at 0° and inclined at angle Φ to the interface. The asymptotic field for a 90° crack was investigated by Cook and Erdogan;[15] however, both materials at the interface were isotropic. Anisotropic cases, therefore, should be examined using the Finite Element Iterative Method. This method is currently a very desirable procedure (see below).

Other singularities of concern are free-edge and corner singularities. the corner singularity problem was raised as a design issue by Adams.[16,25] The results for corner singularity without and with an interface crack will be given. In addition, nonlinear material effects at the corner singularity is investigated using the method discussed in Ref. 14.

V THE FINITE ELEMENT ITERATIVE METHOD (FEI)M

The Finite Element Iterative Method (FEIM)[1-4] was originally developed for evaluating fields in elastic media. The method relies on the use of general-purpose finite element programs in performing the iterations on the circular mesh shown in Figure 1c. The calculation of these iterations is similar to the usual substructuring procedure. The results of the iterations are then analyzed as discussed in Refs. 3 and 4 and the asymptotic field as well as the stress intensities are calculated. As discussed in Ref. 3, the method evaluates the eigenvalue problem solution of a transfer matrix obtained from the stiffness matrix of the domain in Figure 1c. The FEIM can be applied to two- and three-dimensional singularities as well as to any form of material anisotropy at the interface. The method was recently extended to the nonlinear regime of power law hardening materials.[14] In this case, the method seeks the asymptotic field or eigenfunctions of the tangent transfer matrix which can depend on the loading.

VI INTERFACE CRACKS

Although joints made with adherends having prepared surfaces are expected to show cohesive failure, Mode I test results performed on FM300, Ref. 17, showed adhesive, as well as mixed cohesive-adhesive failure. In Mode II loading, which represents a major application of adhesive joints, adhesive cracks (interfacial cracks) are present even if the primary failure is cohesive. It is noted here that, if the behavior is elastic, a cohesive crack in Mode II will have to bend rather than continue to grow in a linear fashion. Plastic behavior would only affect the angle of crack branching. Therefore, it is expected that different proportions of mixed cohesive-adhesive failure will exist, depending on the surface preparation, the environmental effects and the amount of plasticity.

Zero degree interfacial cracks associated with adhesive failure are, therefore,

fundamental for Mode II and mixed-mode testing, the design of joints, and for adhesive failures due to poor surface preparation, as well as for the understanding of micromechanics of surface preparation effects. Interface cracks (adhesive failure) could also be prominent in the presence of high temperature and humidity.

The elastic case of an interface crack for an isotropic material has occupied a great deal of the literature for the past 25 years.[18–21] For anisotropic media, although the eigenfunction method has been used,[22] currently the FEIM approach has proved to be more general in addition to being readily available for the designer and experimental investigator.

The asymptotic field for a general interface crack has the following displacement (u_j) and stress (σ_{1m}) forms,

$$u_j = R_e\{(k_1 + ik_2)r^{(\alpha+i\varepsilon)}[F_j(\Theta) + iG_j(\Theta)]\} \tag{1}$$

$$\sigma_{lm} = R_e\{(k_1 + ik_2)r^{(\alpha-1+i\varepsilon)}[P_{lm}(\Theta) + iQ_{lm}(\Theta)]\} \tag{2}$$

where $i = \sqrt{(-1)^{1/2}}$ and R_e is the real part of the function in parentheses. The above field is a general form for the singularity at interfaces. For a 0° interface crack of a bimaterial elastic medium, α is equal to 1/2. when $\varepsilon = 0$ the field is non-oscillatory, otherwise if $\varepsilon \neq 0$, the stress field has large oscillations as $r \to 0$, which can be seen by expanding Eq. (2),

$$\begin{aligned}\sigma_{lm} = r^{\alpha-1}\{&[k_1 \cos(\varepsilon \ln r) - k_2 \sin(\varepsilon \ln r)]P_{lm}(\Theta) \\ &- [k_1 \sin(\varepsilon \ln r) + k_2 \cos(\varepsilon \ln r)]Q_{lm}(\Theta)\}\end{aligned} \tag{3}$$

The displacement field, Eq. (1), also indicates that in a region very close to the crack tip, closure and maybe material overlap will occur. The latter is not physically feasible and is due the elastic and linear assumptions of the problem. Eqs. (1–3) give a good representation of the field remote from the crack tip region.

A major aspect of this field is that both Modes I and II are always combined even if the remote loading is not. Such a behavior is not only mathematical but leads to the zigzag nature of the crack propagation observed in testing, as discussed in Figure 1. It is also responsible for part of the scatter of the results found in Ref. 7, in addition to the variations in specimen preparation and other parameters which are purely random in nature as discussed above.

i Elastic interface crack

Figures 4 and 5†, respectively, show results for the elastic asymptotic field of a 0° interfacial crack (adhesive failure) of an epoxy adhesive which is

† The stress ordinates in Figures 4–14 are for an arbitrary loading and were not normalized by the yield stress or the stress intensity factor. Only the relative values and distributions are of interest. Similarly, the radial distance r from the crack tip is dimensionless and does not relate to physical dimensions of the specimen.

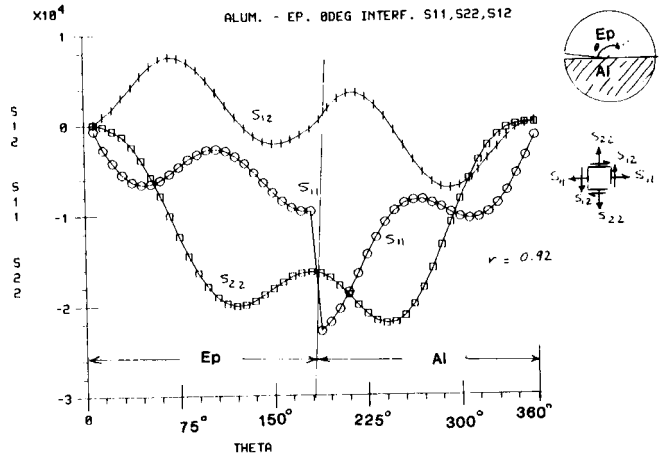

FIGURE 4 Stress field for singular FEIM analysis of an interface crack between epoxy adhesive on aluminum adherend. Phase angle change ($\alpha = 0.5$, $\varepsilon = 0.0669$). See footnote on page 159.

bonded to either aluminum or to a unidirectional glass reinforced epoxy composite As expected, the real part of the singularity is the same for both cases ($\alpha = 1/2$). On the other hand, it is clear from the stress distribution and the singularity of the field (see Table II) that one cannot use fracture results obtained from tests with one adherend and apply them to another. Even for the same adherend material, the direction of the anisotropy will affect the field significantly.

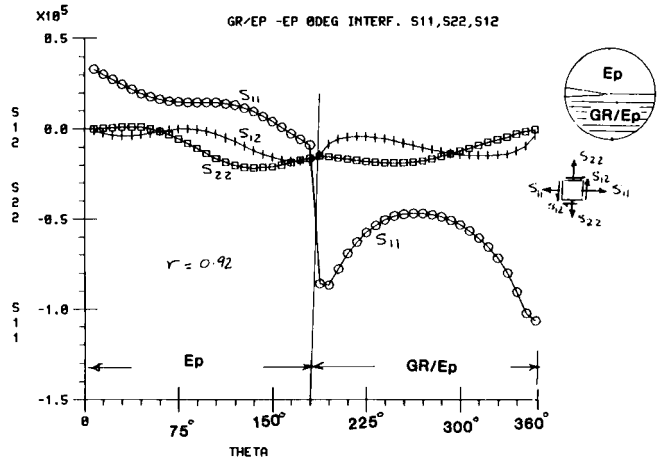

FIGURE 5 Stress field for singular FEIM analysis of an interface crack between epoxy adhesive on graphite/epoxy (0) adherend. Phase angle change ($\alpha = 0.5$, $\varepsilon = 0.0511$). See footnote on page 159.

ii Nonlinear material behavior at interface crack

The asymptotic solution for an interface crack in a nonlinearly hardening material has been recently obtained by FEIM.[14] It is presented here for the hardening power of 3 and 9 which identifies a range of behavior for many ductile adhesives of the class of the high temperature FM300 (American Cyanimid) and the plasticized or modified expoxy adhesives. The nonlinear behavior of these materials is assumed to be of the Ramberg-Osgood form,

$$Ee = a\sigma + (\sigma/\sigma_0)^n \tag{4}$$

where E is the modulus of elasticity, e the strain, σ the stress, a and σ_0 are constants and n is the hardening power. In Ref. 14 it was shown that the asymptotic field depends on the hardening power in a manner similar to the HRR-field for homogeneous materials.[12,13] In addition, it was shown that the field depends on the mode of loading and size of the plastic zone in relation to the distance from the crack tip. The field was found to be represented by the form of Eqs. (1) and (2); however α, ε and the rest of the functions are dependent on a dimensionless distance R_p, which is the ratio of the distance from the crack tip to the end of the region of interest divided by the overall plastic zone size.† Therefore, the asymptotic field can be written as:

$$u_j(R_p) = R_e\{(k_1^p + ik_2^p)r^{(\alpha_p + i\varepsilon_p)}[F_j^p(\Theta) + iG_j^p(\Theta)]\} \tag{5}$$

$$\sigma_{lm}(R_p) = R_e\{(k_1^p + ik_2^p)r^{(-\alpha_p - i\varepsilon_p)}[P_{lm}^p(\Theta) + iQ_{lm}^p(\Theta)]\} \tag{6}$$

Table I gives the values of α_p and ε_p for various values of R_p. When $\varepsilon_p = 0$, practically, the field does not change any more for a region closer to the crack tip. However, the distances at which that occurs are extremely small such that they could be of the order of atomic distances.

The asymptotic field for an interface crack of a power law hardening material is, therefore, more complicated than the HRR-field for homogeneous materials, which is independent of the relative distances from the crack tip. In the interface

TABLE I
Interface singularity for power law hardening material

Power (n)	$1/(1+n)$	R_p	α_p	ε_p
3	1/4	1	0.253	0.0675
		10^{-2}	0.260	0.0655
		10^{-4}	0.280	0.0554
		10^{-6}	0.295	0.0405
		10^{-8}	0.280	0.0000
9	1/10	1	0.106	0.0829
		10^{-2}	0.139	0.0700
		10^{-4}	0.154	0.0000
Elastic	1/2	—	0.5	0.0935

† Using the same approach, the HRR-field for a homogeneous material was found to be independent of R_p, which agrees with the analytical solution of Ref. 12 and 13.

crack case, one has to evaluate the asymptotic field for every application or test. The Finite Element Iterative Method (FEIM) offers a practical approach for characterizing the field.

The practical implications of the results presented above requires the evaluation of the asymptotic field represented by Eqs. (5) and (6), at the same relative material distances (R_p), in both the test specimen where the fracture parameters (J-integral, or strain energy density) are measured and in the application where the fracture is being predicted. The selection of R_p could be based on micromechanical dimensions (material), or on practical dimensions where measurements could be made accurately. It could be concluded from the above results that, as in the elastic case of interface cracks, interfacial adhesive fracture will always involve mixed-mode failure (Modes I and II) unless one is concerned with extremely small distances from the crack tip.

It should be noted here, that although the above results deal with a rigid substrate, they represent for all practical purposes the behavior of most adherends with respect to ductile adhesives (e.g. FM300). Therefore, the results for the asymptotic field shown here, and in Ref. 14, will represent most of the applications of adhesives. If, however, anisotropy of the adherend is of importance, it has to be included in the finite element model used in the FEIM as discussed above or in Ref. 14. The cross-ply modulus or the plasticity of the matrix could also affect the field.

VII. INCLINED INTERFACE CRACKS

Currently, there is no general analytical expression for elastic media with inclined cracks at interfaces. As stated earlier, this problem is fundamental to the investigation of crack propagation and the micromechanics of failure at interfaces. Presented here are some of the results that were obtained from FEIM for an expoxy adhesive which is bonded to either aluminum or graphite/epoxy composite adherends. The material properties used in the analysis were,

Adhesive:	$\nu = 0.35,$	$E = 0.45 \times 10^6$ psi
Adherend:		
Aluminum	$\nu = 0.30,$	$E = 10 \times 10^6$ psi
Gr/Ep	$\nu_{12} = \nu_{13} = 0.3,$	$\nu_{23} = 0.54$
	$E_{12} = 20 \times 10^6,$	$E_{22} = E_{33} = 1.4 \times 10^6$ psi
	$G_{12} = 0.8 \times 10^6,$	$G_{23} = 0.6 \times 10^6$ psi

The asymptotic field is in the same form as Eqs. (1) and (2). The values of α and ε depend on the angle of inclination Φ of the crack to the interface which are given in Table II. Figures 6–8 show the stresses for a crack at inclination $\Phi = 45°$ to the adhesive/aluminum interface. It is clear that the stresses are non-oscillatory in contrast to the case of an 0° interface crack.

TABLE II
Inclined interface crack

Expoxy adhesive—aluminum adherend Angle of crack Φ	α	ε
90°	0.658	0.000
45°	0.561	0.000
30°	0.560	0.000
22.5°	0.570	0.0478
0°	0.500	0.0669
Epoxy adhesive—graphite/epoxy adherend **Angle of crack** **Φ**	**α**	**ε**
45°	0.536	0.000
0°	0.500	0.0511

At $\Phi = 0°$, Williams[18] has shown analytically that in order to satisfy the governing equations for a crack at a bimaterial interface, the displacement function has to be of the form of Eqs. (1–3), with $\varepsilon \neq 0$. On the other hand, for a crack at $\Phi = 90°$ to the bimaterial interface, it was shown in Ref. 15 that the governing equations are satisfied with $\varepsilon = 0$, which is similar to singularities in homogeneous materials.

In the FEIM, Eq. (1) is used and the singularity $(\alpha + i\varepsilon)$ is calculated from the characteristic equation, Ref. 4. If the roots of the characteristic equation are real, then $\varepsilon = 0$, if they are complex, then $\varepsilon \neq 0$. For cracks at any angle Φ, other than 90° and 0°, there is a transition from real to complex singularity at Φ_c. This angle Φ_c is a function of the material properties of the adhesive and adherend and their anisotropy. For the epoxy adhesive to aluminum interface the transition angle

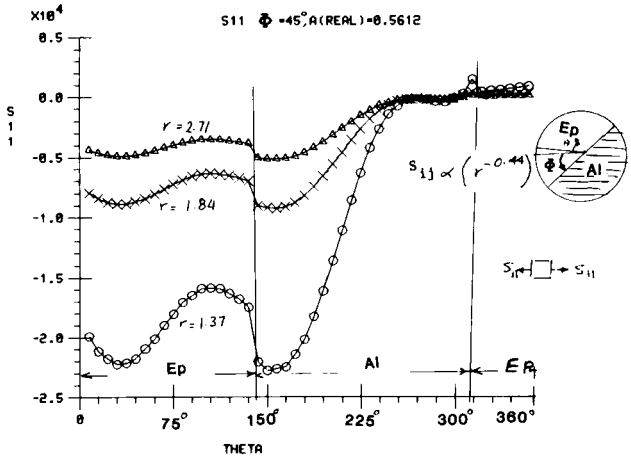

FIGURE 6 Stress distribution (σ_{11}) at various radii from the crack tip for a 45° interface crack (epoxy adhesive/aluminum adherend). No phase angle change ($\alpha = 0.561$, $\varepsilon = 0$). See footnote on page 159.

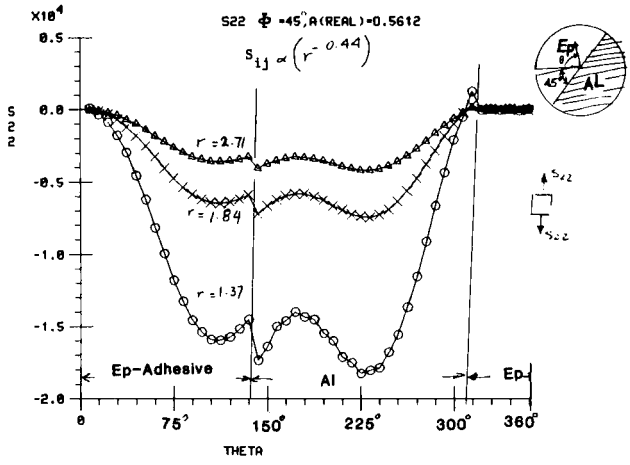

FIGURE 7 Stress distribution (σ_{22}) at various radii from the crack tip for a 45° interface crack (epoxy adhesive/aluminum adherend). No phase angle change ($\alpha = 0.561$, $\varepsilon = 0$). See footnote on page 159.

occurs in the range $30° > \Phi_c > 22.5°$. Therefore, since $\varepsilon > 0$ for $\Phi \leq \Phi_c$, the stresses are oscillatory.

In the above analysis, if the maximum principal stress is used as a criterion for crack propagation, then from Figures 6 and 7 it can be predicted that the crack would propagate along the Ep/Al interface before changing direction.

VIII CORNER SINGULARITY—ADHESIVE INTERFACE

The corner singularity at an adhesive interface is an important problem for joint design.[16] In evaluating the asymptotic field for corner singularity it is essential to

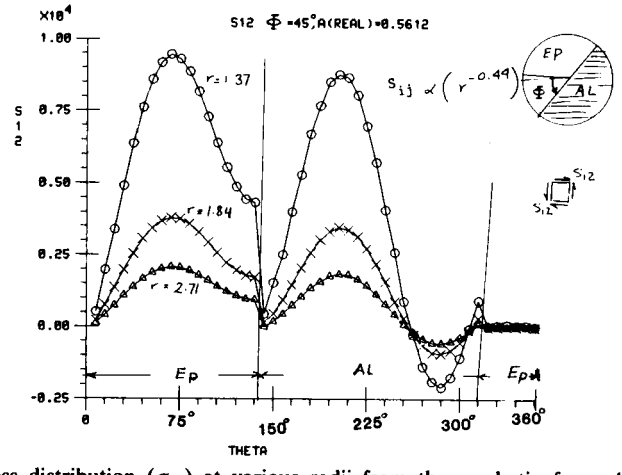

FIGURE 8 Stress distribution (σ_{12}) at various radii from the crack tip for a 45° interface crack (epoxy adhesive/aluminum adherend). No phase angle change ($\alpha = 0.561$, $\varepsilon = 0$). See footnote on page 159.

consider the anisotropy of the adherend. Again, the FEIM is well suited to perform this analysis. For simplicity, the results for a rigid interface for both the elastic and nonlinearly hardening adhesives are presented in this paper.

i Elastic adhesive at rigid corner

This case has been solved by Bogy and Wang[23] and the results can be obtained directly from graphs in their paper which are, however, difficult to read in the region of interest. Solutions are also available from equations given in the paper, but they are complicated to solve. The FEIM was applied to two cases: a square rigid corner and an obtuse angle rigid corner. Both these cases have been investigated experimentally.[26] The results for the square corner are given in Figures 9–11, and the asymptotic field obtained is in the form,

$$\sigma_{ij} = K_1 r^{-0.21} f_{ij}(\Theta) + K_2 r^{-0.41} g_{ij}(\Theta) \tag{7a}$$

The singular field for the 135° rigid corner with the same adhesive properties is given by:

$$\sigma_{ij} = K_1 r^{-0.11} f_{ij}(\Theta) + K_2 r^{-0.28} g_{ij}(\Theta) \tag{7b}$$

The higher singularity in the most general loading cases of the above equations will dominate the field, *i.e.* the second term will be the dominant term. However, for a symmetric loading about the corner the first term will dominate. The results in Figures 9–11 are for this symmetric case.

From Eqs. (7) it is clear that the obtuse angle notch gives a much weaker singularity and hence the greater failure load; this was observed in Ref. 26. In

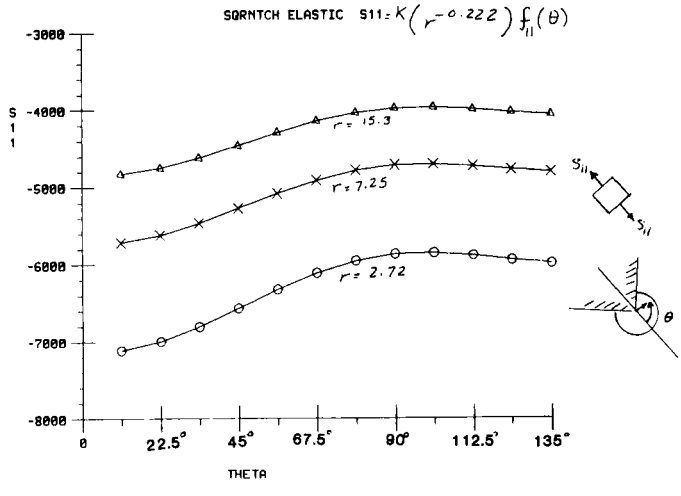

FIGURE 9 Elastic-stress field for corner singularity in an epoxy adhesive. Stresses σ_{11} at various distances from the corner. See footnote on page 159.

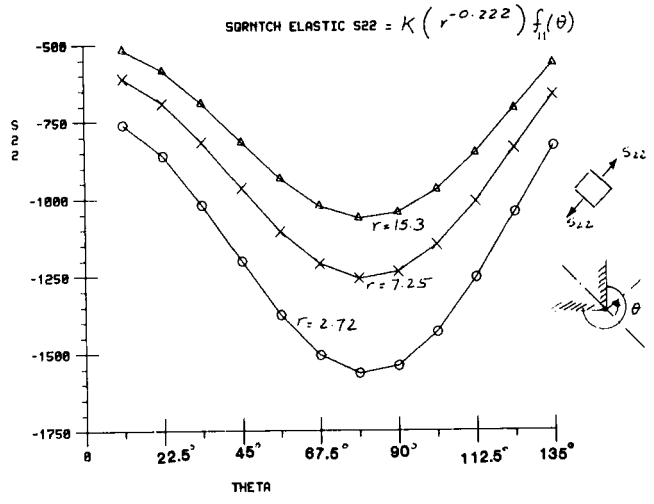

FIGURE 10 Elastic-stress field for corner singularity in an epoxy adhesive. Stresses σ_{22} at various distances from the corner. See footnote on page 159.

Eq. (7), the stress intensities (K_i) can not be used alone to compare the results of two cases because the singular fields are different.

ii Nonlinearly hardening adhesive at a square rigid corner

The procedure discussed in Ref. 14 and in section VI for interface cracks was applied to this case. The adhesive behavior was assumed to follow Eq. (4) with

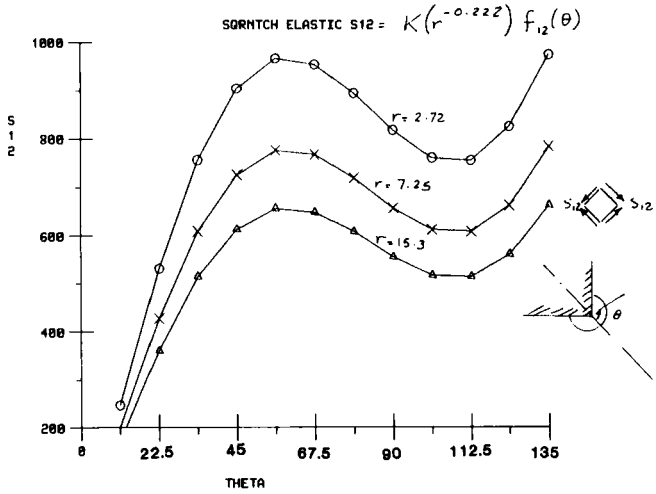

FIGURE 11 Elastic-stress field for corner singularity in an epoxy adhesive. Stresses σ_{12} at various distances from the corner. See footnote on page 159.

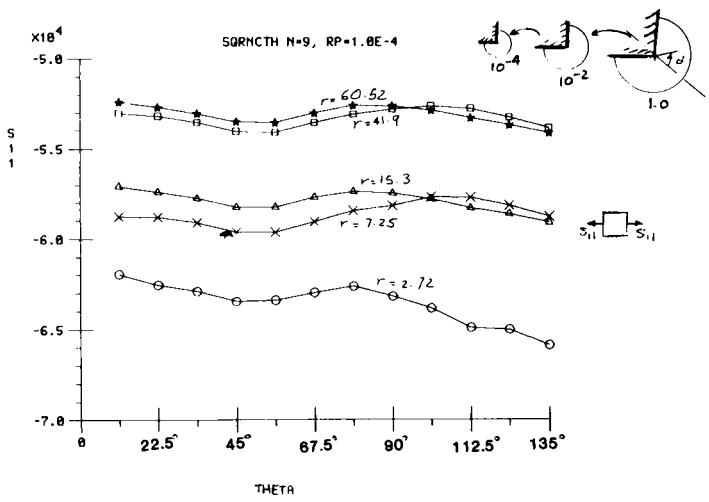

FIGURE 12 Plastic-stress field for corner singularity in an epoxy adhesive ($n = 9$). Stresses σ_{11} at various distances from the corner. Nonseparable field. See footnote on page 159.

$n = 0$, which corresponds to toughened epoxy adhesives. Figures 12 and 13 show the distribution of the stresses at various radii from the singularity. When the FEIM was applied to this field, convergence was not obtained. As discussed in Ref. 14, the lack of convergence of FEIM indicates that the asymptotic field cannot be described by a separable form. Therefore, Eqs. (5–7) or other forms of separable singularities cannot represent that field. On the other hand the strain energy density, shown in Figure 14, was found to behave as,

$$\sigma_{ij}\varepsilon_{ij} \to r^{-0.19} \tag{8}$$

In this case, if the stress field is chosen to be approximated by a power singularity

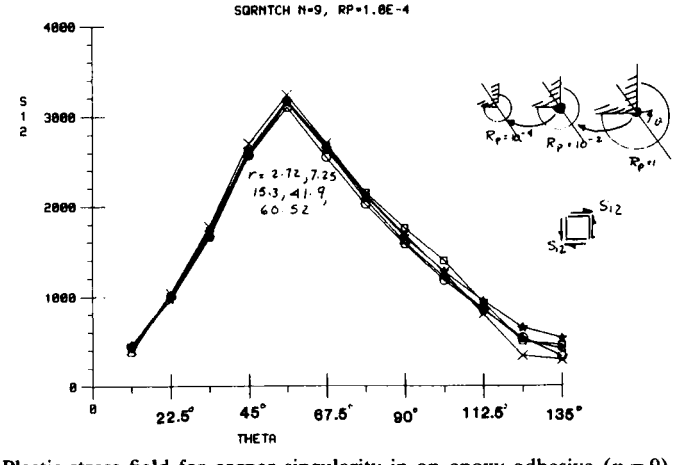

FIGURE 13 Plastic-stress field for corner singularity in an epoxy adhesive ($n = 9$). Stresses σ_{12} at various distances from the corner. Nonseparable field. See footnote on page 159.

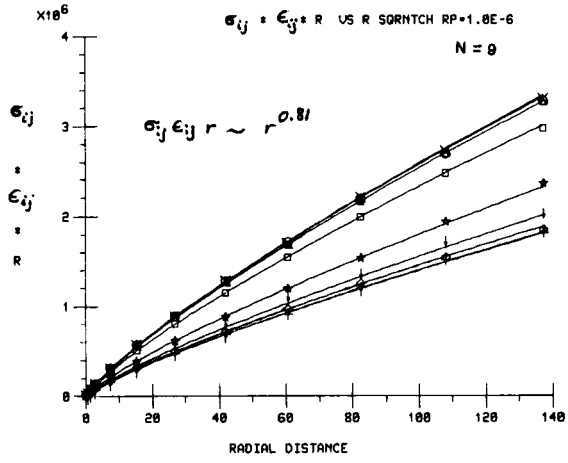

FIGURE 14 Plastic-strain energy density for corner singularity in an epoxy adhesive ($n = 9$). Curve fitting of $\sigma_{ij} \cdot \varepsilon_{ij} \cdot r$ at various angles vs. radial distance. See footnote on page 159.

as in Eqs. (7), then the FEIM together with Eq. (8) give a stress singularity which varies between -0.02 and -0.12 for each variation. Assuming an HRR-field,[12,13] for $n = 9$, the singularity in the stress is given by $[-(1/(1+n)) = -0.1]$. This value, as expected, is near the upper bound of the results obtained by FEIM. It is noted here that Ref. 24 develops a diffrent formula for the singularity using a heuristic approach combined with the HRR-field.

iii Crack at a corner

As discussed above this case, shown in Figure 15, is of importance to design and micromechanics of failure. The asymptotic field was found by applying the FEIM to be represented by:

$$\sigma_{lm} = R_e\{(k_1 + ik_2)r^{(-0.66-i0.036)}[P_{lm}(\Theta) + iQ_{lm}(\Theta)]\} \tag{9}$$

which shows a stronger singularity than a crack in a homogeneous material or a crack at a straight interface. Of course, a singularity in plane strain greater than 0.5 is not admissible from J-integral arguments. However, this field satisfies the finite strain energy requirement (as $r \to 0$ the strain energy density singularity is less than 2). Therefore, Eq. 9 can represent a very strong initiation site for adhesive joints with defects near the square corner. The case of a 135° corner was also analyzed and the stress singularity was found to be

$$\sigma_{lm} = R_e\{(k_1 + ik_2)r^{(-0.4-i0.018)}[P_{lm}(\Theta) + iQ_{lm}(\Theta)]\} \tag{10}$$

which is oscillatory with the real part less than 0.5 and a small imaginary part ε, which could be ignored for all practical purposes.

The singularity results in Eqs. (9) and (10) explain what Adams[25] found from

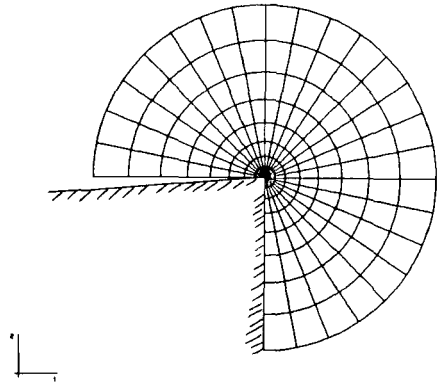

FIGURE 15 Finite element mesh for crack and corner singularities. FEIM results in ($|\alpha - 1| > 0.5$).

his finite element analysis, and the experimental results of Kinloch[26] which were presented at this Conference. They found that an obtuse angle corner joint adherend had three times the failure strength of that of the square corner adherend. Therefore, a square corner adherend with any pre-existing flaw will lead to adhesive failure before any cohesive failure ($r^{-0.5}$ singularity) could be initiated.

CONCLUSIONS

The Finite Element Iterative Method was applied to several problems involving the micromechanics of failure and design of adhesive joints. It was shown that that the singularity is oscillatory when cracks are inclined at angles less than Φ_c, where ($30° > \Phi_c > 22.5°$), in a manner similar to interfacial cracks. Results also indicated that the oscillatory exponent for aluminum is stronger than for the graphite/epoxy composite adherend, thus the mixture of Mode I and II is larger. The degree of mixture of modes can be considered a rationale for the resulting scatter in the G_{Ic} and G_{IIc} data.

The case of a crack singularity combined with a square-corner singularity was shown to be stronger than that of an obtuse angle corner. This was shown to correlate with some recent test results presented at this Conference[25,26]. The results discussed in this paper include also singularities at interfaces of nonlinear materials, zero-degree interface cracks and square-corner singularities. The results of this research are pertinent to the understanding of micromechanics of adhesive failure.

References

1. R. S. Barsoum, *Int. J. of Fract.* **32,** 59–67 (1985).
2. R. S. Barsoum, *Proc. 4th Int. Conf. Num. Meth. in Fract. Mech.*, San Antonio, TX, 23–27 March 1987.

3. R. S. Barsoum, *Int. J. Num. Meth. in Eng.* **25,** 531–539 (1988).
4. R. S. Barsoum, *ibid.* **25,** 541–554 (1988).
5. J. K. Strovier, K. J. Ninow, K. L. DeVries and G. P. Anderson, *Adhesion Science Review,* H. F. Brinson, J. P. Wightman and T. C. Ward, Eds., VA Tech. Ctr. Adh. Sci., Blacksburgh, VA, 1987.
6. K. M. Liechti, T. Hayashi, this Conference.
7. E. Sancaktar, *Proc. 5th. Int. Jt. Mil./Gov.-Ind. Symp. on Struct. Adh. Bond.,* ARDEC, Picatinny Ars., 3–5 Nov. 1987.
8. T. Freda, MS Thesis, Univ. of Texas, Aug. 1987.
9. R. A. Everett, Jr., and W. S. Johnson, in *Delamination and Debonding of materials,* **ASTM STP 876,** 267–281 (1985).
10. C. Arah, *et al., Proc. 5th Inter. Joint Military/Government-Industry Symp. on Struct. Adhesive Bonding,* U.S. ARDEC, Dover N.J., 3–5 Nov. 1987.
11. A. J. Kinloch and S. J. Shaw, J. Adhesion **12,** 59–77 (1981).
12. J. R. Rice and G. F. Rosengren, *J. Mech. Phys. of Solids* **16,** 1–12 (1968).
13. J. W. Hutchinson, *ibid.* **16,** 13–31 (1968).
14. R. S. Barsoum "Sing. Behv. near an Interf. Crack Tip of Power Law Hard. Mat.", Sub. for Publ.
15. T. S. Cook and F. Erdogan, *Int. J. Engg. Sci.* **10,** 667–697 (1972).
16. R. D. Adams and J. A. Harris, *Int. J. Adhesion and Adhesives* **7,** No. 2, 69–80 (1987).
17. S. Mall and W. S. Johnson, in *Composite Materials; Testing and Design,* **ASTM STP 893,** 322–334 (1986).
18. M. L. Williams, *Bull. Seismol. Soc. of Am.,* **49,** 199–204 (1959).
19. J. R. Rice and G. C. Sih, *J. Appl. Mech.* **32,** 418–423 (1965).
20. A. H. England, *ibid.* **32,** 400–402 (1965).
21. M. Cominou, *ibid.* **44,** 631–636 (1977).
22. S. S. Wang and I. Choi, *ibid.* **50,** 179–183 (1983).
23. D. B. Bogy and K. C. Wang, *Int. J. Solids and Struct.* **7,** 993–1005 (1971).
24. H. L. Groth, Discussion Ref. 16, *Int. J. Adhesion and Adhesives,* **8,** No. 1, 55–56 (1988).
25. R. D. Adams, this Conference.
26. A. J. Kinloch, this Conference.